



40th IABSE Symposium, 19-21 September 2018, Nantes, France.  
Tomorrow's Megastructures

## Fibre Reinforced Geopolymer versus Conventional Reinforced Concrete layers for the structural strengthening of RC beams

**Mohammed Haloob Al-Majidi**

*School of Environment and Technology, University of Brighton, UK*

*Department of Civil Engineering, College of Engineering, University of Basrah, Basrah, Iraq*

**Andreas Lampropoulos**

*School of Environment and Technology, University of Brighton, UK*

**Andrew Cundy**

*School of Ocean and Earth Science, University of Southampton, Southampton SO14 3ZH, UK.*

**Ourania Tsioulou**

*School of Environment and Technology, University of Brighton, UK*

**Salam Alrekabi**

*Department of Civil Engineering, Al-Mustaqbal University College, Babylon, Iraq*

Contact: [a.lampropoulos@brighton.ac.uk](mailto:a.lampropoulos@brighton.ac.uk)

### Abstract

A common technique used to increase the flexural capacity of RC beams is the external application of RC layers. In this case, crucial parameter for the efficiency of the examined technique is the connection between the new layer and the existing concrete, since lack of sufficient connection at the interface may lead to premature failure of the strengthened elements. Another crucial parameter for the durability of the strengthened elements is the corrosion of the reinforcement of the layers. In the current study, fibre reinforced geopolymer concrete layers reinforced with steel bars were used for the flexural strengthening of reinforced concrete beams. Accelerated corrosion tests were conducted followed by flexural loading. The results indicate that, the addition of fibre reinforced geopolymer concrete offers improved load performance and durability, since higher maximum load increment was observed and the effect of corrosion was found to be negligible.

**Keywords:** fibre reinforced geopolymer concrete, corrosion, strengthening, layers.

## 1 Introduction

The structural strengthening of existing structures is an urgent need worldwide and especially in earthquake prone areas either because the existing structures are damaged, or because they have been designed without the implementation of seismic codes or using old code provisions. One of the most widely used strengthening technique is the addition of Reinforced Concrete (RC) layers or jackets to RC structures and it has been proved that this technique can considerably improve the structural performance of existing elements [1,2]. In this case, it is crucial to ensure that sufficient connection is provided at the interface between the old and the new RC elements [1]. Another crucial parameter for the structural performance of the strengthened elements is the durability and the corrosion of the steel reinforcement. When the concrete cover is not sufficient, chloride ions penetrate the cover concrete and reach the steel bars, leading to destruction of the passive film and subsequent corrosion of the steel bars which significantly affects the structural performance of the RC elements [3-5].

In the last two decades, the addition of steel fibres to the concrete mix has been extensively studied in order to improve the mechanical performance and especially the ductility and the post-cracking performance of conventional concrete, and high performance cementitious materials such as the Ultra High Performance Fibre Reinforced Concrete (UHPFRC) have been developed. The addition of UHPFRC layers has been proved to be quite efficient for the flexural and shear strengthening of existing structural elements [6, 7].

The development of Fibre Reinforced Geopolymer Concrete (FRGC) has also been studied in previous research projects as an alternative sustainable and environmental friendly material with enhanced mechanical performance and strain hardening characteristics [8, 9].

In this study, FRGC layers reinforced with steel bars were used for the structural strengthening of RC beams. Acceleration corrosion was applied to the steel bars of the additional layers prior to the testing of the beams using impressed current

method. Additional elements with conventional concrete and without accelerated corrosion were also examined in order to evaluate the effectiveness of the examined technique.

## 2 Experimental investigation and specimens preparation

In this section, the geometry and the dimensions of the examined specimens are presented alongside with the material properties and description of the FRGC preparation.

### 2.1 Description of the examined specimens

In this study, eight beams were examined in total. Four beams were strengthened with Normal Strength Conventional concrete (NSC); two with induced accelerated corrosion to the steel bars of the layer (NSC-S-corr) and two without corrosion (NSC-S). Another four specimens were strengthened with Polyvinyl-Alcohol Fibre Reinforced Geopolymer Concrete (PVAFRGC) layers; two with induced accelerated corrosion to the steel bars of the layer (PVAFRGC-S-corr) and two without corrosion (PVAFRGC-S).

For the initial beams, two bars of 10 mm diameter ( $2\Phi 10$ ) and 530 MPa yield stress were placed in the tensile side (Figure 1). Stirrups of 8 mm diameter ( $\Phi 8$ ) and 350 MPa yield stress were used in the shear span at an interval of 90 mm. Ordinary Portland Cement was used for the casting of the initial beams with mean cube compressive strength at the day of testing equal to 32 MPa.

The additional layer was cast 3 months after the casting of the initial beams. The surface of the initial beams was roughened using air chipping hammer to a depth of 2-3 mm. The thickness of the additional layer was equal to 50 mm and the layers were reinforced with two bars of 10 mm diameter ( $2\Phi 10$ ) and 530 MPa yield stress (Figure 1).

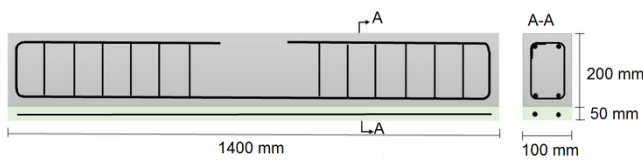


Figure 1. Geometry of the strengthened beams

## 2.2 PVAFRGC and NSC layer preparation

For the PVAFRGC, Fly Ash (FA) was used together with Ground Granulated Blast Furnace Slag (GGBS) and undensified Silica Fume (SF). Silica sand with maximum particle size of 500  $\mu\text{m}$  was also used in this mix. Potassium hydroxide and potassium silicate solution were used as activators. Regarding the fibres, 2% (by volume) Polyvinyl-Alcohol (PVA) fibres of 12 mm length were added to the mix. For the NSC, a conventional cement based mix with similar estimated strength characteristics to the PVAFRGC was used. Both mix proportions for PVAFRGC and NSC are presented in Table 1.

Table 1. Mix compositions for PVAFRGC and NSC

| Material           | Mix proportions [Kg/m <sup>3</sup> ] |     |
|--------------------|--------------------------------------|-----|
|                    | PVAFRGC                              | NSC |
| Fly ash            | 388                                  | -   |
| Slag               | 310                                  | -   |
| Silica fume        | 78                                   | -   |
| Cement             | -                                    | 380 |
| Alkaline activator | 93                                   | -   |
| Water              | 194                                  | 194 |
| Sand               | 1052                                 | 920 |
| Gravel             | -                                    | 800 |
| PVA fibre          | 26                                   | -   |

For the mixing of the materials, Zyklos high shear mixer (Pan Mixer ZZ 75 HE) was used. Geopolymer binder (FA, GGBS, and SF) was placed first in the mixer, followed by alkaline liquid, and sand. The liquid phase was prepared in advance by mixing potassium silicate solution with water and polycarboxylate based superplasticizer for 5 min prior to mixing with the solid phase. The materials were dry mixed for 5 min and then the liquid phase was added and the mixer run for a further 5

min. After that, fibres were gradually added after sieving through an appropriate steel mesh at the top of the mixer, in order to ensure uniform fibre dispersion in the geopolymer mix. Finally, sand was added to the mixer, and the mixer run for another 3 min to give a total mixing time of 13 min.

After demoulding, the samples were covered with plastic sheets to prevent moisture loss and were cured at room temperature up to the testing date. The mechanical characteristics for both NSC and PVAFRGC were obtained from standard compressive tests of cubes with 100mm side and direct tensile tests of dog bone specimens with cross section 13 mm x 50 mm.

Based on the results of these tests, the compressive and tensile strength of PVAFRGC were found equal to 46 MPa and 3.5 MPa, while the respective values for NSC were found equal to 43 MPa and 3 MPa, which confirms that similar material properties were achieved for these two different materials used for the additional layers.

## 2.3 Accelerated corrosion

Impressed current technique was used to simulate the effect of corrosion on the steel reinforcement of the additional layer (Figure 2).

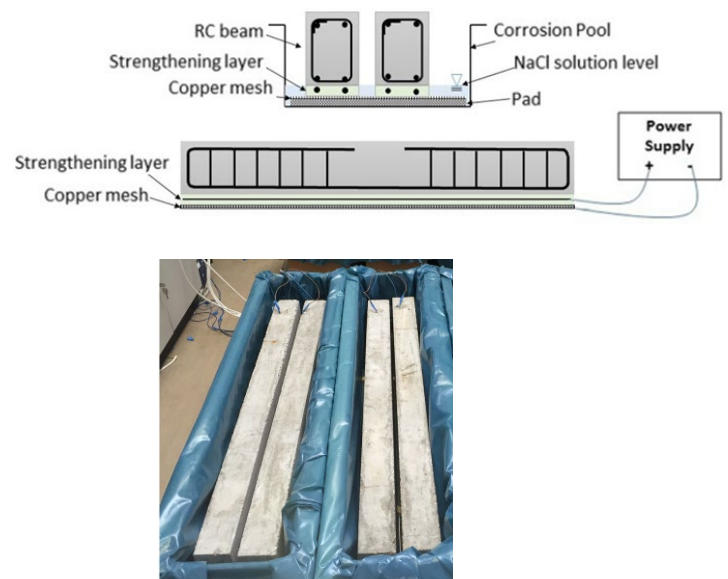


Figure 2. Accelerated corrosion setup

A constant current of 300 mA was applied for 30 days between the reinforcement bars (anode) of

the additional layer and a copper mesh (cathode) at the bottom surface of the container which was connected to the negative terminal of a DC power supply (Figure 2).

### 2.4 Four-point bending tests

For the evaluation of the structural performance of the strengthened beams, four-point bending tests were conducted and the load versus mid-span displacement was recorded. In addition to the load-deflection results, Linear Variable Displacement Transducers (LVDT) were used to monitor the slip at the interface between the layers and the initial beams (Figure 3).



Figure 3. Four-point bending setup

The effective span in all the examined specimens was equal to 1200 mm and the specimens were tested under displacement control with a loading rate of 0.004 mm/s.

## 3 Results and discussion

After the end of the four-point loading tests, the bars of the corroded specimens were used to evaluate the effect of the corrosion by measuring the mass loss, alongside with the experimental results of the bending tests.

### 3.1 Load versus deflection results and evaluation of the effect of corrosion

The failure mode and the crack pattern during the four point bending tests of the strengthened beams with reinforced NSC layers are presented in Figure 4, while the respective results for the beams strengthened with reinforced PVAFRGC layers are presented in Figure 5.

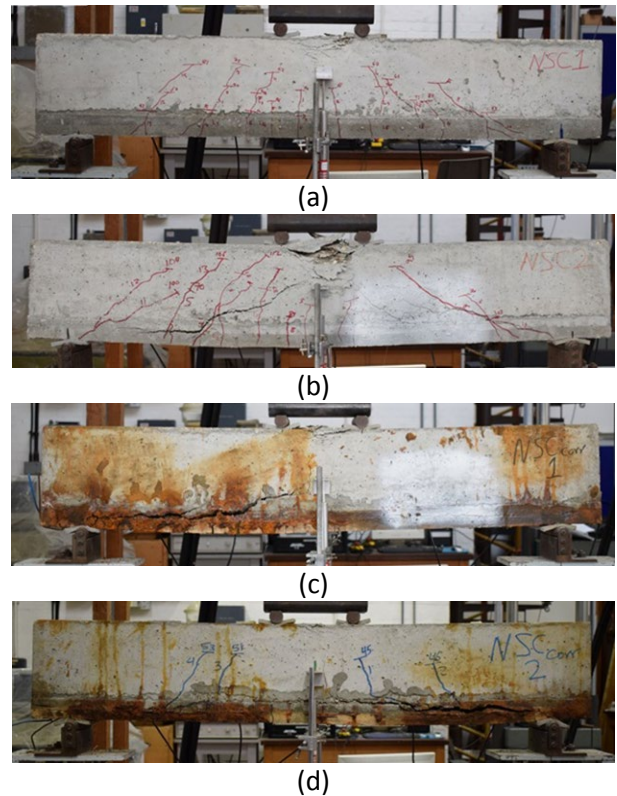


Figure 4. Failure mode of beams a) NSC-S-1, b) NSC-S-2, c) NSC-S-corr-1, and d) NSC-S-corr-2

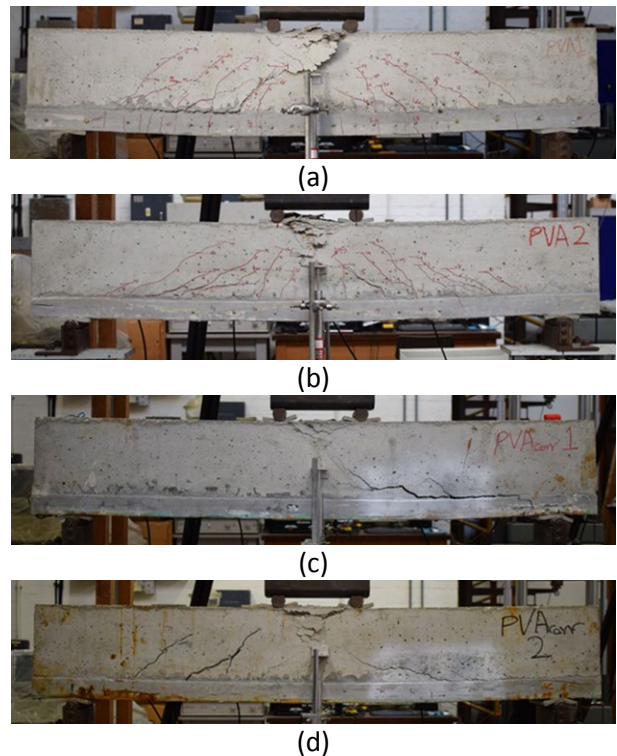


Figure 5. Failure mode of beams a) PVAFRGC-S-1, b) PVAFRGC-S-2, c) PVAFRGC-S-corr-1, and PVAFRGC-S-corr-2

The failure modes of Figure 4a and Figure 4b indicate that, in case of RC beams strengthened with NSC layers without corrosion, concrete crushing occurred first followed by shear cracks and cracks at the interface. In case of the corroded specimens (Figure 4c and Figure 4d) peeling off of the concrete cover layer occurred together with interface cracks after the shear cracks, which is attributed to the severely damaged concrete layer due to corrosion. The specimens strengthened with PVAFRGC layers (Figure 5) had overall similar failure mode with the specimens strengthened with NSC layers with the main difference that in case of specimens strengthened with PVAFRGC layers, there was not any separation of the concrete cover of the corroded specimens (Figure 4c and Figure 4d) which confirms the improved corrosion resistance of PVAFRGC. In most of the examined specimens (Figure 4 and Figure 5) cracks occurred at the interface at some point near the maximum load value.

The load versus deflection results for the specimens strengthened with reinforced NSC and PVAFRGC layers are illustrated in Figure 6 and Figure 7 respectively.

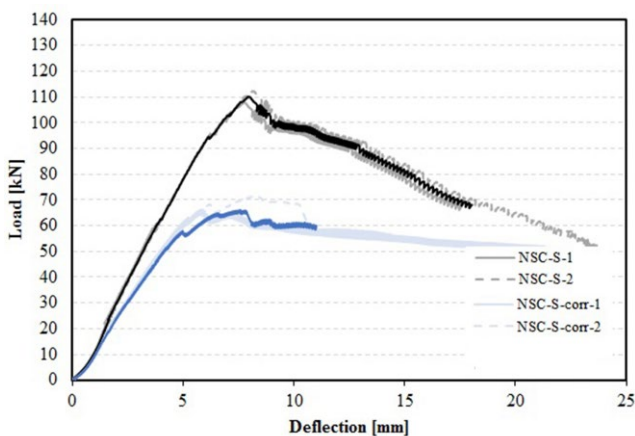


Figure 6. Load versus deflection results for beams strengthened with reinforced NSC layers

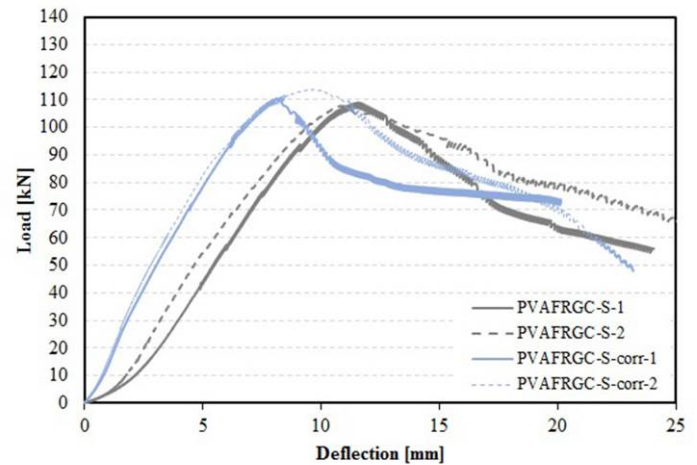


Figure 7. Load versus deflection results for beams strengthened with reinforced PVAFRGC layers

Based on the results of Figure 6, the average maximum load of the beams strengthened with NSC without corrosion was found equal to 109.5 kN, while the respective value for the corroded specimens was considerably lower and equal to 68.7 kN which corresponds to a 37 % reduction. In case of beams strengthened with PVAFRGC layers (Figure 7) the average maximum load of the non-corroded specimens was found equal to 106.9 kN while the respective value for the corroded specimens was found to be very similar and equal to 112.1 kN. This indicates that the corrosion did not affect the maximum load value and confirms the beneficial effect of the PVAFRGC layer on the corrosion resistance of the strengthened specimens.

In order to further evaluate the effect of the degree of corrosion, the reinforcement bars were mechanically cleaned using a stiff metal brush in order to remove any adhering corrosion products and the mass loss was measured. The mass loss in case of specimens strengthened with NSC was found equal to 11% while the respective reduction of specimens strengthened with PVAFRGC was found significantly lower and equal to 7.5% which confirms the beneficial effect of the PVAFRGC for the protection of the steel bars towards corrosion.

### 3.2 Evaluation of the interface conditions

The interface slip was measured during the testing of all the examined specimens and these values were used for the evaluation of the interface characteristics.

Using the slip measurements of the RC beams strengthened with NSC overlay, the maximum interface slip ( $s_{max}$ ) at the ultimate load ( $P$ ) together with the load values for slip equal to 0.2 mm ( $P_{s=0.2}$  mm), 0.8 mm ( $P_{s=0.8}$  mm), and 1.5 mm ( $P_{s=1.5}$  mm) are presented in Table 2. These slip values (0.2 mm, 0.8 mm and 1.5 mm) are the maximum slip values adopted by the Greek Code of Structural Interventions [10] for immediate occupancy, life safety and collapse prohibition behaviour levels.

Table 2. Load and slip values at various loading stages

| Specimen         | P [kN] | $s_{max}$ [mm] | $P_{s=0.2}$ mm [kN] | $P_{s=0.8}$ mm [kN] | $P_{s=1.5}$ mm [kN] |
|------------------|--------|----------------|---------------------|---------------------|---------------------|
| NSC-S-1          | 106.8  | 1              | 60.0                | 87.0                | --                  |
| NSC-S-2          | 112.2  | 0.69           | 60.7                | --                  | --                  |
| NSC-S-corr-1     | 66.1   | 0.32           | 45.7                | --                  | --                  |
| NSC-S-corr-2     | 71.3   | 1.33           | 36.8                | 65.7                | --                  |
| PVAFRGC-S-1      | 109.0  | 0.70           | 57.9                | 109.0               | --                  |
| PVAFRGC-S-2      | 104.7  | 0.41           | 67.4                | --                  | --                  |
| PVAFRGC-S-corr-1 | 110.5  | 0.82           | 80.1                | 80.6                | --                  |
| PVAFRGC-S-corr-2 | 113.6  | 0.6            | 79.3                | --                  | --                  |

Based on the results of Table 2, it can be observed that overall lower slip values were measured at the maximum load for specimens strengthened with PVAFRGC layers, compared to the respective values of specimens strengthened with NSC layers. An average maximum slip value equal to 0.63 mm was measured at the maximum load for all the four specimens strengthened with PVAFRGC layers, which is quite lower, compared to the respective average load for the specimens strengthened with NSC layers which was found equal to 0.84 mm. This indicates improved

interface conditions in case of specimens strengthened with PVAFRGC layers.

The interface shear strength ( $\tau_{fud}$ ) of the strengthened RC beams can be simplified estimated using the model proposed by the Greek Code of Structural Interventions [10] for roughened interface (Eq.1).

$$\tau_{fud} = \begin{cases} 0.25 \cdot f_{ct}, & \text{smooth interface} \\ 0.75 \cdot f_{ct}, & \text{rough interface} \\ f_{ct}, & \text{use of shotcrete} \end{cases} \quad (1)$$

Where:  $f_{ct}$  is the tensile strength of the concrete with the lower strength (between the old and the new concrete).

Also, the respective interface shear stress ( $\tau_x$ ) can be determined according to the British standard BS 8110-1 [11] using Eq. 2, and the respective results for the examined specimens are presented in Table 3.

$$\tau_x = \frac{V_{sd}}{b \cdot z} \quad (2)$$

Where:

$V_{sd}$  is the shear force of the examined section of the beam,

$b$  is the width of the interface, and

$z$  is the lever arm of the composite section.

Table 3. Interface shear strength and stress values

| Specimen         | $\tau_{fud}$ [MPa] | $\tau_x$ (for $P_{max}$ ) [MPa] | $\tau_x$ (for $P_{s=0.2}$ mm) [MPa] |
|------------------|--------------------|---------------------------------|-------------------------------------|
| NSC-S-1          | 1.51               | 2.67                            | 1.50                                |
| NSC-S-2          | 1.51               | 2.80                            | 1.52                                |
| NSC-S-corr-1     | 1.51               | 1.65                            | 1.14                                |
| NSC-S-corr-2     | 1.51               | 1.78                            | 0.92                                |
| PVAFRGC-S-1      | 1.51               | 2.73                            | 1.45                                |
| PVAFRGC-S-2      | 1.51               | 2.62                            | 1.69                                |
| PVAFRGC-S-corr-1 | 1.51               | 2.76                            | 2.00                                |
| PVAFRGC-S-corr-2 | 1.51               | 2.84                            | 1.98                                |

Based on the results of Table 3, the shear stress at the maximum load ( $\tau_x$ ) was higher than the shear strength ( $\tau_{fud}$ ) for all the examined specimens and this is in agreement with the experimental

observations which show interface slips and cracks during the bending tests (Figure 4 and Figure 5). For corroded specimens strengthened with NSC (NSC-S-corr-1 and NSC-S-corr-2) shear stress values were significantly lower compared to the respective values for the non-corroded specimens (NSC-S-1 and NSC-S-2) which is attributed to the reduced load capacity of the corroded specimens.

#### 4 Conclusions and recommendations

In this paper, experimental investigation was conducted in order to evaluate the efficiency of the use of additional PVAFRGC reinforced layers for the improvement of the mechanical performance and durability of strengthened RC beams and comparisons were presented with respective specimens strengthened with conventional RC layers.

Based on the results of this study the following conclusions can be drawn:

- In case of specimens strengthened with PVAFRGC layers, the mass loss of the steel bars due to the corrosion was found significantly lower compared to the respective mass loss of the specimens strengthened with NSC layer, which shows improved resistance of PVAFRGC towards steel corrosion.
- From the load-deflection results it was evident that, in case of specimens strengthened with reinforced NSC layers, the maximum load was significantly reduced due to the corrosion while, in case of specimens strengthened with PVAFRGC layers, there was not any reduction in the maximum load due to the effect of the corrosion.
- Based on the interface slip values measured during the bending tests, overall lower maximum slip values were observed in case of specimens strengthened with reinforced PVAFRGC layers, compared to the respective results of specimens strengthened with reinforced NSC layers. This indicates improved interface conditions of the

specimens strengthened with PVAFRGC layers.

Overall, from the experimental results presented in this study, it is evident that the application of reinforced PVAFRGC layer for the strengthening of existing RC elements can offer improved resistance to corrosion and significantly enhanced structural performance.

#### 5 References

- [1] Tsioulou, O., Lampropoulos, A., and Dritsos, S. Experimental investigation of interface behaviour of RC beams strengthened with concrete layers. *Construction and Building*. 2013; **40**: 50-59.
- [2] Cheon, H., and MacAlevey, N. Experimental behaviour of jacketed reinforced concrete beams. *ASCE Journal of Structural*. 2000; **126**: 692-699.
- [3] Kobayashi, K., and Rokugo, K. Mechanical performance of corroded RC member repaired by HPRCC patching. *Construction and Building Materials*. 2013; **39**: 139-147.
- [4] Rajamane, N., Nataraja, M., Lakshmanan, N., and Dattatreya, J. Rapid chloride permeability test on geopolymer and Portland cement. *Indian Concrete Journal*. 2011: 21-26.
- [5] Ahmad, S. Techniques for inducing accelerated corrosion of steel in concrete. *The Arabian Journal for Science and Engineering*. 2009; **34**: 95-104.
- [6] Lampropoulos, A., Paschalis, S., Tsioulou, O., and Dritsos, S. Strengthening of reinforced concrete beams using ultra high performance fibre reinforced concrete (UHPFRC). *Engineering Structures*. 2016a; **106**: 370-384.
- [7] Bastien Masse, M., Brühwiler, E. Contribution of R-UHPFRC Strengthening layers to the shear resistance of RC elements. *Structural Engineering International*, 2016; **4**: 365-374
- [8] Al-Majidi, M. H., Lampropoulos A., and Cundy, A. Tensile properties of a novel fibre reinforced geopolymer composite

- with enhanced strain hardening characteristics. *Composite Structures*. 2017; **168**: 402-427.
- [9] Al-Majidi, M. H., Lampropoulos A., and Cundy, A. Steel fibre reinforced geopolymer concrete (SFRGC) with improved microstructure and enhanced fibre-matrix interfacial properties. *Construction and Building Materials*. 2017; **139**: 286-307.
- [10] Greek Code of Structural Interventions. Earthquake Planning and Protection Organization. Athens, Greece; 2013.
- [11] BS 8110-1. Structural use of concrete. Part 1: Code of practice for design and construction. ed. London: British Standard Institute; 1997.